

Global scale-invariant dissipation in collisionless plasma turbulence

K. H. Kiyani,^{1,*} S. C. Chapman,¹ Yu. V. Khotyaintsev,² and M. W. Dunlop³

¹Centre for Fusion, Space and Astrophysics; University of Warwick, Coventry, CV4 7AL, United Kingdom

²Swedish Institute of Space Physics, Uppsala, Sweden

³Rutherford Appleton Laboratory, Didcot, United Kingdom

A higher-order multiscale analysis of the dissipation range of collisionless plasma turbulence is presented using *in-situ* high-frequency magnetic field measurements from the Cluster spacecraft in a stationary interval of fast ambient solar wind. The observations, spanning five decades in temporal scales, show a crossover from multifractal intermittent turbulence in the inertial range to non-Gaussian monoscaling in the dissipation range. This presents a strong observational constraint on theories of dissipation mechanisms in turbulent collisionless plasmas.

PACS numbers: 94.05.Lk, 52.35.Ra, 96.60.Vg, 95.30.Qd

The solar wind provides an ideal laboratory for the study of plasma turbulence [1]. *In-situ* spacecraft observations suggest well-developed turbulence at 1 AU with a magnetic Reynolds number $\sim \mathcal{O}(10^5)$ [2, 3]. These show an inertial range of Alfvénic turbulence on magnetohydrodynamic (MHD) scales which is an anisotropic and possibly compressible energy cascade [4, 5, 6] with intermittent magnetic field fluctuations described by statistical multifractals and a power spectral density (PSD) with a scaling exponent close to $-5/3$ [1]. An outstanding problem is how, in the absence of collisional viscosity in the solar wind, this inertial range of MHD turbulence terminates at smaller scales where one anticipates a cross-over to dissipative and/or dispersive processes via wave-particle resonances. Understanding the nature of the dissipation processes may also inform open questions such as how the solar wind and solar coronal plasmas are heated [7, 8, 9].

It has long been known [10, 11] that in collisionless plasmas there is a transition in the PSD at high wavenumber k from MHD to kinetic physics at approximately the ion gyroscale. High resolution *in-situ* magnetic field observations reveal that at these scales the turbulent solar wind shows a transition from a $\sim -5/3$ power law in the inertial range to a steeper power-law at higher k with spectral exponents in the range $(-4, -2)$ [12, 13]. However, the relevant physical mechanism is much debated; having implications for phenomena as diverse as magnetic reconnection [14, 15], neutron stars and accretion disks [16]. Theories which have been proposed range from nonlinear turbulent-like cascade processes [17, 18, 19] to weak turbulence theories with wave dispersion and resonant plasma interactions [20]. As well as studies of *in-situ* spacecraft measurements in the solar wind [21], foreshock [22] and magnetosheath [23, 24] regions, these theories are explored using simulations ranging from Hall-MHD [25], electron-MHD [16, 26], gyrokinetics [27], particle-in-cell simulations of whistler turbulence [28] and Vlasov-hybrid simulations [29].

Both neutral fluid and MHD turbulence share a ‘classic’ statistical signature – namely an intermittent mul-

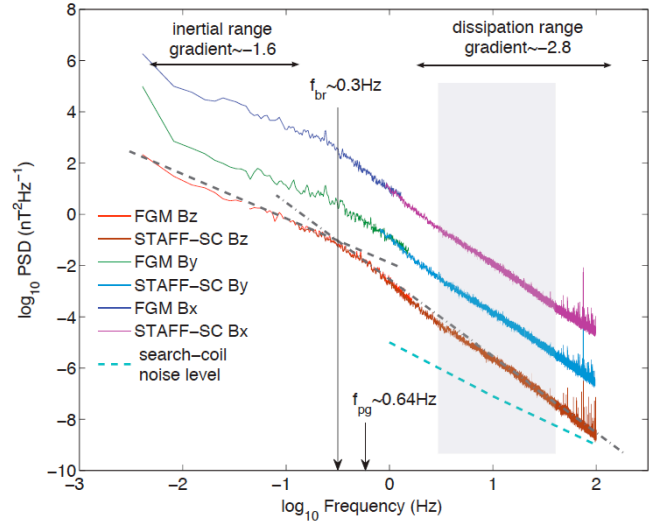


Figure 1: PSD plots of the components of the magnetic field from both FGM (at frequencies lower than 1 Hz) and STAFF-SC (at frequencies above 1 Hz) instruments. The PSD values for B_x and B_y have been shifted up for clarity. The 95% confidence intervals for all these plots are at $\pm 0.03 \log_{10} nT^2 Hz^{-1}$. The shaded region denotes the frequency range of STAFF-SC to be studied; the upper limit corresponds to the search-coil signal-to-noise ratio (SNR) of 10dB; the lower limit to the SNR of 20dB [30]. At lower frequencies the STAFF-SC response is attenuated by the instrument calibration filter.

tifractal scaling seen in the higher-order statistics. In this letter we test the statistical properties of the dissipation range and find in contrast monoscaling behaviour i.e. a global scale-invariance. This provides a strong discriminator for the physics and phenomenology of the dissipation range in collisionless plasmas.

We present a detailed analysis of an interval of quiet, stationary solar wind observed *in-situ* by the Cluster spacecraft quartet during an hour interval 00:10 – 01:10 UT on January 30, 2007. By combined analysis using high-frequency measurements of magnetic field fluctuations from the search-coil (STAFF-SC) [31] and flux-gate

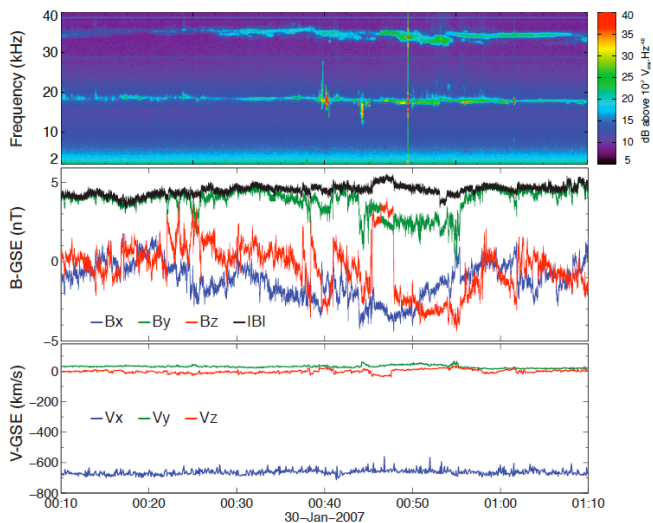


Figure 2: Summary plot illustrating the quiet nature of the solar wind interval under study. Top panel: E-field spectrogram from WHISPER on Cluster spacecraft 4 showing steady plasma emissions; center panel: B-field components; bottom panel: ion velocities from HIA on Cluster spacecraft 1.

magnetometers (FGM) [32], we simultaneously probe both the inertial range and dissipation range up to frequencies of 80 Hz. This will allow us to establish the scaling properties in the dissipation range over about two decades in frequency. Figure 1 shows the overlaid PSD from FGM and STAFF-SC for our interval for the three magnetic field components B_x , B_y and B_z in geocentric ecliptic (GSE) coordinates – both the inertial and dissipation ranges can be clearly seen in all three components. We indicate on the plot the frequency corresponding to the Doppler-shifted proton gyroradius f_{pg} [19] which is close to the cross-over frequency break f_{br} between the inertial and dissipation range. A summary of the solar wind interval used in this study is shown in fig. 2. We plot the electric field spectrogram in a frequency range 2 – 40 kHz from WHISPER [33], the magnetic field timeseries from FGM and the ion velocity from CIS/HIA [34] during the interval of interest. The constant ion velocity and plasma density (evidenced by the constant electron plasma frequency on the E-field spectrogram) indicate a stationary pristine interval of ambient solar wind disconnected from the Earth’s bowshock, away from ion and electron foreshock regions and imbedded in a steady fast solar wind stream $\gtrsim 650 \text{ km s}^{-1}$ *i.e.* quintessential plasma turbulence away from any external *a priori* physical processes and dynamics. Due to stationarity of plasma parameters and the B-field magnitude it is sufficient to quote single values for the other relevant parameters: ion temperature $T_i \simeq 1.2 \text{ MK}$, Alfvén speed $V_A \simeq 50 \text{ km s}^{-1}$, ion plasma beta $\beta \simeq 2$, and plasma density $n_e \simeq 3.8 \text{ cm}^{-3}$ (from the plasma frequency measured by WHISPER).

Importantly for this study, we have chosen an inter-

val where both STAFF-SC and FGM were operating in *burst-mode* so that one can access the largest range of scales available and probe further into smaller scales where the dissipation range can be studied. For this interval STAFF-SC provides AC waveform data in a frequency band between $\sim 0.1 \text{ Hz}$ and 180 Hz (low-pass filter); our study is restricted to frequencies lower than 80 Hz to maintain good SNR. FGM provides DC waveform data with largest frequency at $\sim 33 \text{ Hz}$ (Nyquist cutoff). This ensures a large sample ($\sim 1.6 \times 10^6$ for STAFF-SC and $\sim 2.5 \times 10^5$ for FGM) and thus well-resolved statistics. The Welch PSD method used in fig. 1 employs 50% overlapped windows each containing a sample of 2^{14} points for FGM and 2^{16} points for STAFF-SC; this provides a very large range of frequencies to study as well as reducing the error due to noise on the PSD measurements. The large sample size coupled with the intervals stationarity ensures that we have a good control of errors which can arise due to finite sample size [35]. All the results presented in this paper are from Cluster spacecraft 4; the B_z component provides the largest overlap in frequencies between both FGM and STAFF-SC due to it being out of the spin plane of the spacecraft and thus is cleanest with respect to spin tone contamination. As we will be studying single point Eulerian measurements in very fast solar wind, streaming past the spacecraft providing a single time-series, we will assume the validity of Taylor’s frozen-in-turbulence hypothesis [23] which uses time as a proxy for space – although our PSD and other statistics will always be presented in the frequency and time domains.

The PSD provides one statistic to probe the scale dependent behaviour of the turbulent fluctuations and is equivalent to studying the autocorrelation – a second order statistic. To test for multifractal scaling of the fluctuations we now turn to higher-order statistics. We focus on the statistics of magnetic field increments defined as $\delta B_i(t, \tau) = B_i(t + \tau) - B_i(t)$ for each vector component i and time lag or scale τ ; in particular the focus is on the absolute moments of these increments, also known as structure functions

$$S_i^m(\tau) = \frac{1}{N} \sum_{j=1}^N |\delta B_i(t_j, \tau)|^m, \quad (1)$$

where m is the moment order. We have verified the statistical stationarity of the interval being studied and thus can form an ensemble average by taking a time average (assuming ergodicity) along the signal of sample size N . Importantly, the higher-order structure functions progressively capture the more intermittent, larger fluctuations. As we are studying the magnetic field increments, these large fluctuations represent the spatial gradients which are responsible for dissipating energy from the magnetic fields. We will focus on the scaling be-

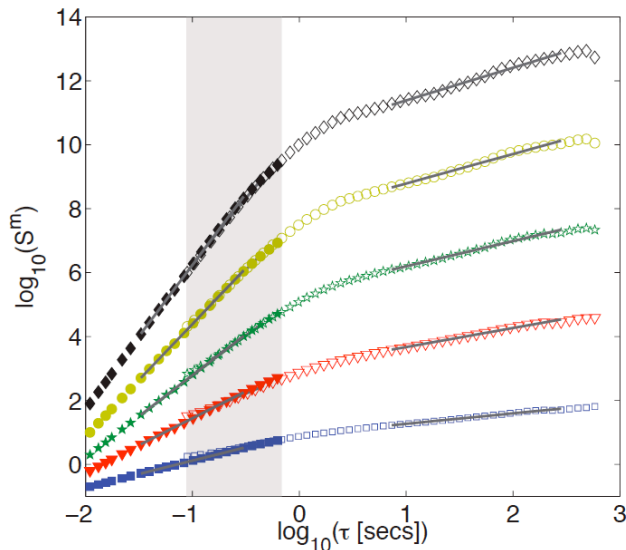


Figure 3: Structure functions of orders: 1- \square , 2- ∇ , 3- \star , 4- \circ and 5- \diamond . Open shapes correspond to FGM measurements and filled shapes refer to STAFF-SC. The curves have been shifted along the vertical axis to allow a comparison of the gradients. The shaded area indicates the scales where both FGM and STAFF overlap. Linear fits for the inertial and dissipation ranges are also shown.

haviour of the structure functions with scale τ such that

$$S_i^m(\tau) \propto \tau^{\zeta(m)}, \quad (2)$$

where linear dependence of the scaling exponent $\zeta(m) = Hm$ implies monoscaling with a single exponent H . In theories of turbulence non-linear $\zeta(m)$ behaviour is associated with the intensity of energy dissipation being distributed on a spatial multifractal [1].

The structure functions for the data interval studied here are shown in fig. 3. On this $\log - \log$ plot the gradients as shown give estimates of the scaling exponents $\zeta(m)$. The inertial and dissipation ranges of scaling are well-defined with a sharp transition at the break point at $\simeq 3$ seconds in agreement with the PSD in fig. 1; the dissipation range extends over nearly two orders of magnitude. Importantly, there is excellent agreement between STAFF-SC and FGM in the dissipation range where they overlap for almost a decade, indicated by the shaded region on the plot. We plot $\zeta(m)$ vs. m for the dissipation range in the main panel of fig. 4, and for the inertial range in the inset. Surprisingly, the dissipation range is monoscaling i.e. globally scale-invariant; in contrast to the inertial range which is multifractal, characteristic of fully developed turbulence with $\zeta(2) \sim 2/3$. The single scaling parameter for the dissipation range for B_z is $H = 0.89 \pm 0.02$ for STAFF-SC and $H = 0.84 \pm 0.05$ for FGM. To test the robustness of this result we have repeated this analysis for another ambient fast solar wind interval (12:10 – 14:00 UT January 20, 2007) and obtained the same global scale-invariance. In both cases we

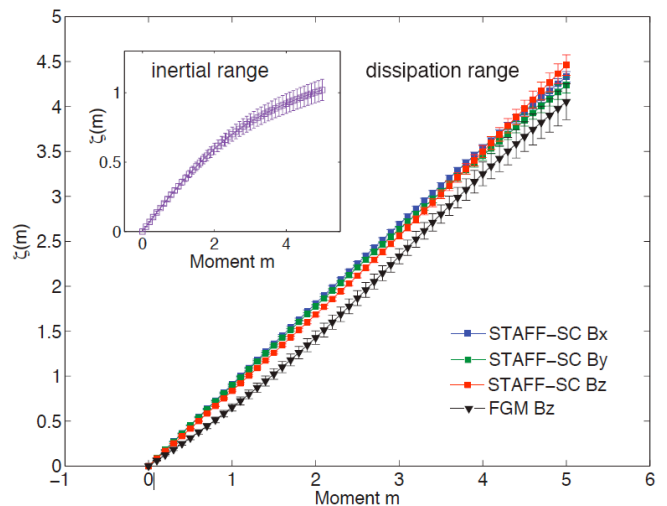


Figure 4: Main plot: Scaling exponents ζ with order m ; a linear relationship on this plot indicates monoscaling behaviour. $\zeta(m)$ obtained from both FGM and STAFF-SC are shown for B_z ; these show close correspondence. STAFF-SC B_x , B_y components are also shown and indicate isotropic scaling. Inset: $\zeta(m)$ Vs. m for the inertial range using FGM B_z ; this is concave, consistent with the multifractal nature of the inertial range.

find that all three field components are monoscaling. We can see that for the particular solar wind interval shown in fig. 4 the exponents H for B_x and B_y are close to that of B_z , suggesting that the small scale features of this turbulent interval of the solar wind are also isotropic. For STAFF-SC data from the second interval, however, we find $H = 0.9 \pm 0.02$ for B_x and B_y and $H = 0.8 \pm 0.05$ for B_z , suggesting an anisotropy that may depend on local plasma parameters.

Monoscaling of the structure functions implies that the probability density function (PDF) of the increments $P(\delta B_i, \tau)$ at a particular scale τ should collapse onto a unique scaling function \mathcal{P}_s via the following rescaling operation [36]

$$\mathcal{P}_s(\delta B_i \tau^{-H}) = \tau^H P(\delta B_i, \tau). \quad (3)$$

This collapse of the data to a single scaling function is tested in fig. 5 for B_z , where we have used the same values of τ and the H value obtained above. We can see that there is an excellent collapse onto a single curve. A fitted Gaussian illustrates the highly non-Gaussian nature of the tails of this PDF.

In conclusion, our results suggest that global scale invariance in small-scale magnetic fluctuations is a robust feature of the dissipation range of collisionless plasma turbulence in the fast ambient solar wind. This is a surprising result as it is distinct from the multifractal scaling that is characteristic of both neutral fluid and MHD turbulent cascades in the inertial range. Successful theoretical understanding of the dissipation range should include

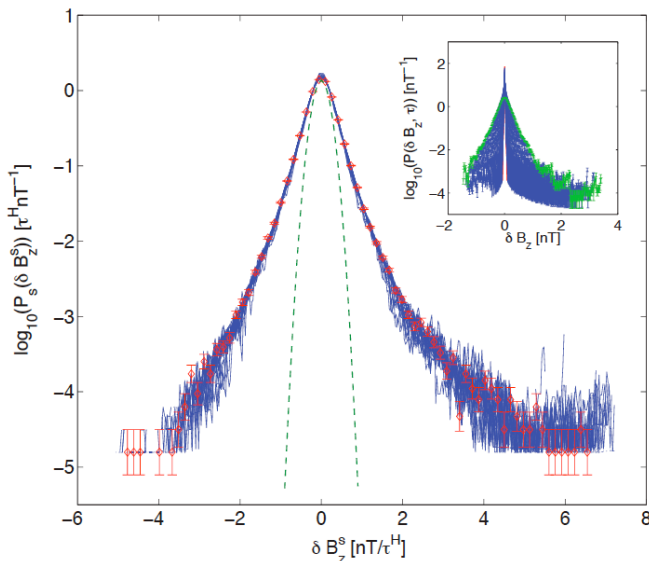


Figure 5: Main plot: PDFs rescaled using eq. (3) ($\delta B_z^s = \delta B_z \tau^{-H}$). Inset: PDFs at different scales τ before rescaling; red and green curves show the smallest and largest values of τ respectively. A Gaussian fit to the data illustrates the heavy-tailed non-Gaussian nature of the rescaled PDF.

this property. Our result provides a strong discriminator of the relevant physics and phenomenology; for example the monoscaling that we find is reminiscent of that found at higher orders in electron-MHD simulations [37]. To determine whether this phenomenology is in fact universal, future studies should aim to reproduce and/or break this result in more dynamic environments such as at planetary shocks [22], magnetosheath [24] and at sites of magnetic reconnection [14, 15]; although the main difficulty here will be to identify sufficiently long stationary intervals.

We thank E. Yordonova, C. Foullon, B. Hnat, ISSI team 132 and in particular T. Dudok De Wit for their help and suggestions; P. Canu and O. Santolik for STAFF-SC calibration queries; N. Cornilleau-Wehrlin, A. Balogh, H. Réme and their teams for use of STAFF-SC, FGM and CIS/HIA data respectively; and P. Décréau and S. Grimald for the WHISPER spectrogram. This work was supported by the UK STFC.

* Electronic address: k.kiyani@warwick.ac.uk

[1] R. Bruno and V. Carbone, *Living Rev. Solar Phys.* **2** (2005).
 [2] W. H. Matthaeus, S. Dasso, J. M. Weygand, L. J. Milano, C. W. Smith, and M. G. Kivelson, *Phys. Rev. Lett.* **95**, 231101 (2005).
 [3] L. Sorriso-Valvo et al., *Phys. Rev. Lett.* **99**, 115001 (2007).
 [4] B. Hnat, S. C. Chapman, and G. Rowlands, *Phys. Rev.*

Lett. **94** (2005).
 [5] S. C. Chapman and B. Hnat, *Geophys. Res. Lett.* **34** (2007).
 [6] T. S. Horbury, M. Forman, and S. Oughton, *Phys. Rev. Lett.* **101**, 175005 (2008).
 [7] R. J. Leamon, W. H. Matthaeus, C. W. Smith, G. P. Zank, D. J. Mullan, and S. Oughton, *Astrophys. J.* **537**, 1054 (2000).
 [8] J. C. Kasper, A. J. Lazarus, and S. P. Gary, *Phys. Rev. Lett.* **101**, 261103 (2008).
 [9] J. A. Araneda, Y. Maneva, and E. Marsch, *Phys. Rev. Lett.* **102**, 175001 (2009).
 [10] P. J. Coleman Jr., *Astrophys. J.* **153**, 371 (1968).
 [11] K. W. Behannon, *Rev. Geophys.* **16**, 125 (1978).
 [12] R. J. Leamon, C. W. Smith, N. F. Ness, W. H. Matthaeus, and H. K. Wong, *J. Geophys. Res.* **103**, 4775 (1998).
 [13] C. W. Smith, K. Hamilton, B. J. Vasquez, and R. J. Leamon, *Astrophys. J.* **645**, L85 (2006).
 [14] D. Sundkvist, A. Retinò, A. Vaivads, and S. D. Bale, *Phys. Rev. Lett.* **99**, 025004 (2007).
 [15] J. P. Eastwood, T. D. Phan, S. D. Bale, and A. Tjulin, *Phys. Rev. Lett.* **102**, 035001 (2009).
 [16] J. Cho and A. Lazarian, *Astrophys. J. Lett.* **615**, L41 (2004).
 [17] S. Galtier and E. Buchlin, *Astrophys. J.* **656**, 560 (2007).
 [18] O. Alexandrova, V. Carbone, P. Veltri, and L. Sorriso-Valvo, *Astrophys. J.* **674**, 1153 (2008).
 [19] F. Sahraoui, M. L. Goldstein, P. Robert, and Yu. V. Khotyaintsev, *Phys. Rev. Lett.* **102**, 231102 (2009).
 [20] R. J. Leamon, W. H. Matthaeus, C. W. Smith, and H. K. Wong, *Astrophys. J. Lett.* **507**, L181 (1998).
 [21] S. D. Bale, P. J. Kellogg, F. S. Mozer, T. S. Horbury, and H. Reme, *Phys. Rev. Lett.* **94**, 215002 (2005).
 [22] Y. Narita, K.-H. Glassmeier, and R. A. Treumann, *Phys. Rev. Lett.* **97**, 191101 (2006).
 [23] F. Sahraoui et al., *Phys. Rev. Lett.* **96**, 075002 (2006).
 [24] O. Alexandrova, C. Lacombe, and A. Mangeney, *Annales Geophysicae* **26**, 3585 (2008).
 [25] D. Shaikh and P. K. Shukla, *Phys. Rev. Lett.* **102**, 045004 (2009).
 [26] D. Biskamp, E. Schwarz, and J. Drake, *Phys. Rev. Lett.* **76**, 1264 (1996).
 [27] G. G. Howes et al., *Phys. Rev. Lett.* **100**, 065004 (2008).
 [28] S. Saito, S. P. Gary, H. Li, and Y. Narita, *Physics of Plasmas* **15** (2008).
 [29] F. Valentini, P. Veltri, F. Califano, and A. Mangeney, *Phys. Rev. Lett.* **101**, 025006 (2008).
 [30] A. Pedersen et al., *Space Science Reviews* **79**, 93 (1997).
 [31] N. Cornilleau-Wehrlin et al., *Space Sci. Rev.* **79**, 107 (1997).
 [32] A. Balogh et al., *Space Sci. Rev.* **79**, 65 (1997).
 [33] P. M. E. Décréau et al., *Space Science Reviews* **79**, 157 (1997).
 [34] H. Reme et al., *Space Science Reviews* **79**, 303 (1997).
 [35] K. H. Kiyani, S. C. Chapman, and N. W. Watkins, *Phys. Rev. E* **79**, 036109 (2009).
 [36] K. Kiyani, S. C. Chapman, and B. Hnat, *Phys. Rev. E* **74**, 051122 (2006).
 [37] G. Boffetta, A. Celani, A. Crisanti, and R. Prandi, *Phys. Rev. E* **59**, 3724 (1999).